





OPEN Urine metabolite profiling in Indian males exposed to high-altitude: a longitudinal pilot study

Manisha Kumari¹, Dolly Sharma¹, Anu Kumari¹, Mallesh Rao Eslavath¹, Chhavi Rai¹, Maramreddy Prasanna Kumar Reddy¹, Lilly Ganju², Rajeev Varshney¹ & Ramesh Chand Meena¹  

People who visit high-altitude for research and development work, pilgrimage, recreational purposes and deployments are exposed to different environmental conditions such as low temperature and atmospheric pressure, leading to hypoxia, high radiation, dry air, and non-availability of fresh food and vegetables. These environmental stressors have significant physiological effects on the human body. Among these challenges, hypobaric hypoxia at high-altitude affects aerobic metabolism and thereby reduces the supply of metabolic energy. Metabolic alterations may further lead to extreme environment related maladaptation as evidenced by alterations in the levels of metabolites and metabolic pathways. To investigate the variation in the metabolite profile, urine samples were collected from 16 individuals at baseline (BL, 210 m) and high-altitude (HA, 4200 m). Untargeted urinary metabolic profiling was performed by liquid chromatography-mass spectrometry (LC–MS) in conjunction with statistical analysis. Univariate and multivariate statistical analyses revealed 33 differentially abundant metabolites based on fold change, VIP score and p value. These distinct metabolites were primarily associated with pathways related to phenylalanine, tyrosine and tryptophan biosynthesis; metabolism of phenylalanine, biotin, tyrosine, cysteine and methionine along with alanine, aspartate and glutamate metabolism. These pathways are also linked with pentose and glucuronate interconversions, citrate cycle, vitamin B6 and porphyrin metabolism. Furthermore, receiver operating characteristic curve analysis detected five metabolites namely, 2-Tetrahydrothiopheneacetic acid, 1-Benzyl-7,8-dimethoxy-3-phenyl-3H-pyrazolo [3,4-c] isoquinoline, Abietin, 4,4'-Thiobis-2-butanone, and Hydroxyisovaleroyl carnitine with high range of sensitivity and specificity. In summary, this longitudinal study demonstrated novel metabolic variations in humans exposed to high-altitude, utilising the potential of LC–MS based metabolomics. Thus, the present findings shed light on the impact of hypoxic exposure on metabolic adaptation and provide a better understanding about the pathophysiological mechanisms underlying high-altitude illnesses correlated to tissue hypoxia.

Keywords Metabolomics, Metabolites, High-altitude, Hypobaric hypoxia, Metabolism, Liquid chromatography-mass spectrometry, Longitudinal

The primary physiological challenges posed by high-altitude (HA) environment is the combination of low oxygen and pressure levels, leading to hypobaric hypoxia (HH), which adversely affects human health. Ascending to HA often results in symptoms such as headache, dizziness, fatigue, insomnia, cognitive impairment and gastrointestinal issues (loss of appetite, nausea and vomiting)¹. The process of adaptation to hypoxia likely to induce variations in biochemical parameters across various biological fluids, leading to shift in metabolites and metabolic pathways. Multiple investigations have been conducted under varying hypoxic conditions to comprehend these metabolic changes. For instance, Gareth et al. documented the activation of pathways linked to lipid, protein, and purine nucleotide metabolism in response to exercise under hypoxic and normoxic conditions; though hypoxia per se did not induce a greater metabolic alterations when compared with normoxia². Another group of researchers reported alterations in several metabolic pathways such as energy, inflammatory response, heme and bile-acid metabolism in healthy individuals in fourth day response of HA (5300 m)³. In

¹Department of Disruptive and Deterrence Technologies, Defence Institute of Physiology and Allied Sciences, Lucknow Road, Timarpur, Delhi 110054, India. ²Research and Development, Malwanchal University, Indore, Madhya Pradesh, India. ✉email: rcmeena.dipas@gov.in; rcmdipas@gmail.com

addition to above, a study scrutinized the metabolomic alterations in the plasma of healthy individuals both prior and during the ascend to Everest Base Camp (5300 m) towards escalating exposure to hypobaric hypoxia. Their findings indicated an increase in glycolytic rate, by virtue of decreased isoleucine and glucose⁴. Gandhi et al.⁵ reported that exposure to chronic environmental hypoxia at Siachen Camp (3700 m) led to alterations in cis-aconitate, tyrosine, nicotinamide mononucleotide, choline and creatinine in urine samples using a ¹H NMR metabolomic technique. Occurrence of acute mountain sickness (AMS) at HA is also very common. Zhu et al.⁶ found that hypoxanthine, cysteinylglycine, D-arabitol, L-allothreonine, 2-ketobutyric acid and succinate semialdehyde in the plasma of AMS patients were increased significantly. Reduced abundance of creatinine detected in human urine and variations in ATP production related pathways may contribute for susceptibility to AMS at HA (4300 m)⁷.

The balance of bio-fluid metabolites within cells and tissues is very intricate, and any disruptions in cellular processes can lead to alterations in the composition of bio-fluid metabolites⁸. Among all bio-fluids, urine stands out as an excellent medium for monitoring dynamic responses to various stimuli^{9,10}. It is a versatile bio-fluid produced by the kidneys, contains a diverse array of compounds, including both endogenous and exogenous substances such as amino acids, fatty acids, lipids, carbohydrates, hormones, peptides, xenobiotics, and metabolic end products like glucuronides and sulfo-conjugates¹¹. It offers several advantages for epidemiological studies as it is plentiful, sterile, and easy to collect biological fluid¹². Urine provides insights into numerous vital functions of the body through the presence of metabolites originating from various primary biochemical processes, reflecting patho-physiological conditions, cardio-metabolic factors, gut microbial metabolism, and short-term dietary intake^{13–15}.

Metabolomics is a powerful technique used for the quantitative differential analysis of metabolite levels in response to pathological, physical, or chemical stimulus including changes in oxygen availability¹⁶. Advancements in chromatography, mass spectrometry, and bioinformatics have enabled metabolomics to conduct “untargeted” screenings, characterizing both known and unknown smaller metabolites (molecular weight < 1500 Da) across various conditions¹⁷. The primary platforms utilized in metabolomics include gas chromatography-mass spectrometry (GC-MS), liquid chromatography-mass spectrometry (LC-MS), and proton nuclear magnetic resonance (¹H NMR). Each platform presents distinct advantages and drawbacks¹⁸. In comparison to the limited sensitivity and extensive sample preparation required for ¹H NMR, as well as the lower throughput of GC-MS due to factors like derivatization, LC-MS offers high sensitivity, increased throughput capacity, and simplified sample preparation. Additionally, the combination of separation techniques, such as chromatography, with MS significantly enhances its ability to analyze highly complex biological samples, positioning LC-MS as one of the most widely utilized platforms in metabolomic research in last decade¹⁹.

Currently, there is a scarcity of scientific literature on metabolic alterations at high-altitudes, and our study differs significantly from previous studies in this area. One notable difference is the ascending height of the participants which was 4200 m, which is greater than that reported in many other studies^{5,7}. This study seeks to fill this gap by identifying alterations in the urine metabolites of human volunteers exposed to hypoxia at HA. To the best of our knowledge, no longitudinal study has been performed on human urinary metabolites at an altitude of 4200 m, and our study the first attempt to assess changes in urinary metabolite profiles in Indian male volunteers of the same ethnicity who are ascended to such extreme altitude. This research further investigated the modulation of metabolic pathways and potential biomarkers. To achieve these objectives, the present study employs an LC-MS based metabolomic approach to analyse the metabolic composition and variations among different study groups through multivariate and pathway analysis techniques.

Materials and methods

Subject recruitment and ethical consent

A total of 16 healthy, male participants aged between 22 and 35 years were recruited for the study. Although our study was designed to be gender-inclusive, no female participants volunteered to take part in the study. Prior to enrolment, individuals underwent comprehensive medical and psychological assessments to exclude any underlying diseases, ensuring the recruitment of a healthy population. None of the participants used any drug or antibiotic that could significantly affect the cellular and biochemical metabolism. All expedition participants understood the nature of the study and we have obtained informed consent from all the volunteers. The article does not contain any information or images that could lead to identification of the study participant and there were no patient or human names were mentioned in the manuscript. Ethical approval for the study was received from Institutional Research Ethics Committee. All other study procedures were carried out in compliance with the principles outlined in the Declaration of Helsinki.

Sample collection

First urine pass from the morning, was collected in sterile urine vials. The initial sample collection took place at the baseline, denoted as BL (210 m). After the BL collection, the participants travelled to different altitudes (3000–4500 m) for acclimatization and reached at HA, 4200 m and the final collection was performed after their stay for one month at HA. Within 1 h of collection, all the samples were immediately treated with sodium azide (2.5 mM), centrifuged for 10 min at 4000 rpm for removal of particles. The samples were immediately distributed in aliquots of 2 ml each and stored at –40 °C. The sample were then transported to base level, stored at –80 °C for further acquisition and analysis.

Sample preparation

200 µL urine sample was combined with 200 µL of acetonitrile, followed by vortexing the mixture for 30 s. Then, the mixture underwent centrifugation at 14,000×g for 10 min at 4 °C. Samples were re-suspended in MeOH:water (1:1, 0.2% formic acid) with 10 µL injection volume. Sample introduction was via UPLC (Dionex

UltiMate 3000). ESI ionization (positive/negative mode) was used with capillary voltage 3.5 kV, source temperature 320 °C, sheath gas 35 psi, and auxiliary gas 10 psi. The mass analyzer (Orbitrap, full scan mode, m/z 100–1000, resolution 70,000 FWHM, accuracy < 2 ppm) ensured high precision. Calibration used LockMass (m/z 445.12003, flow rate 5 $\mu\text{L}/\text{min}$, frequency 30 s), ensuring adherence to Metabolomics Standards Initiative (MSI) guidelines.

Untargeted metabolomics using LC–MS

All LC–MS experiments were carried out using the Dionex UltiMate 3000 UHPLC (Thermo Fisher Scientific, MA, USA) system equipped with a binary solvent delivery manager and a sample manager, coupled with a Thermo Orbitrap Exploris mass spectrometer 240 (Thermo Fisher Scientific, CA, USA) with operating in positive (ESI⁺) and negative (ESI[−]) electrospray ionization mode, separately. Separation was achieved with solvent A [Water + 0.1% (v/v) formic acid] and solvent B [Acetonitrile + 0.1% (v/v) formic acid] with a flow rate of 0.35 mL/min. The total gradient time was set at 16 min with the following gradients: 0 min (2% B), 0–2 min (2% B), 2–5 min (2–20% B), 5–9 min (20–100% B), 9–13 min (100% B), 13–13.1 min (2% B) and 13.1–16 min (2% B). The mass spectrometric data were collected using a Thermo Orbitrap Exploris mass spectrometer.

Data processing and analysis

Pre-processing of the data was performed using Thermo Q Exactive Orbitrap raw files converted to mzML with ProteoWizard (version 3.0). Compound Discoverer (CD) 3.3 (Thermo Fisher Scientific, MA, USA) software was used for workflow-based analysis, including background subtraction, noise reduction, retention time alignment (max shift 0.2 min), and peak picking (min peak intensity 5×10^3 , S/N ratio ≥ 3). Spectral deconvolution was applied to resolve overlapping peaks, and adduct detection (H⁺, Na⁺, K⁺, NH₄⁺) was included for feature annotation. Compound grouping was performed across samples using m/z (mass tolerance 5 ppm) and RT similarity (0.2 min window). For compound consolidation, mass tolerance was set at 5 ppm and retention time (RT) to 0.2 min. Metabolite annotation at Level 2 (putative annotation) was performed through ChemSpider and mzCloud databases. ChemSpider database search was performed with KEGG and Human Metabolome Database²⁰. The analysis results were exported with following filtration criteria: delta ppm range from −5 to +5 ppm. Both positive and negative mode analysis was performed separately, which was combined at later stage and duplicates were removed.

Statistical analysis

MetaboAnalyst 6.0 (<https://www.metaboanalyst.ca/home.xhtml>), an online analysis software was used for statistical analysis, metabolite functional annotation and pathway analysis²¹. We conducted a data normalization process, followed by a principal component analysis (PCA). It was used to supervise holistic metabolomic alterations between BL and HA group participants and to inspect the stability of this study. Furthermore, an orthogonal partial least squares discriminant analysis (OPLS-DA) was employed to distinguish between both the groups and identify significant variables contributing to this classification, utilizing variable importance in projection (VIP) values/score. The t-test statistical analysis was utilized to identify the variance in metabolites between the groups with Benjamini–Hochberg false discovery rate (FDR) to adjust p -value for multiple hypothesis testing. Volcano plots were generated to screen important metabolites with fold change (FC > 2 or < 0.5) between the groups. Then, for the determination of differential metabolites with VIP > 1, FC > 2 or < 0.5, and p -value < 0.05, were considered. Correlation analysis between differential metabolite was performed by Pearson correlation analysis. Metabolic pathway analysis was also done to identify any significant modulation caused by pathophysiological mechanisms associated with acclimatization to hypobaric hypoxia in the HA group's metabolic pathway. Lastly, a receiver operating characteristic (ROC) curve was constructed to assess the discriminatory capability of potential biomarkers in distinguishing between BL and HA group.

Results

Metabolite analysis using LC–MS of human urine samples

The present study demonstrates the untargeted metabolomics of total 32 urine samples of BL and HA conditions through LC–MS techniques. A total of 287 and 353 metabolites were detected in negative and positive modes, respectively. After metabolite annotations from both positive and negative, duplicates were deleted and a total of 391 metabolites were left for analysis (Table S1). Typical total ion current chromatograms in positive ion mode and negative ion mode of LC–MS are shown for BL (Fig. 1a,b) and HA (Fig. 1c,d), where variations can be visually observed between the two urine sample chromatograms.

Metabolic profiling of human exposed to hypobaric hypoxia by LC–MS

At first, unsupervised PCA score plots were generated for the preliminary assessment of urine metabolite profiles which changed significantly as the subjects moved from BL to HA, reflecting the subjects' response to altitude changes. Principal components 1 and 2 (i.e. PC1 and PC2), which accounted for 20.1% and 12.4%, respectively, provided the best group separation (Fig. 2a). To delve deeper into the discriminatory metabolites between the groups, a supervised OPLS-DA model was executed. The score plot revealed a distinct separation between the two groups (Fig. 2b). The OPLS-DA model was cross-validated via a permutation analysis ($n = 20$), and good discrimination was detected between the two groups revealing significant differences in the metabolic profiles of the BL and HA urine samples (Fig. 2c). The OPLS-DA model was evaluated through cross-validation and goodness-of-fit parameters were employed. R²X and R²Y estimate the goodness of fit and Q² is the qualitative measure of the predictive ability of the OPLS-DA model (Fig. 2d).

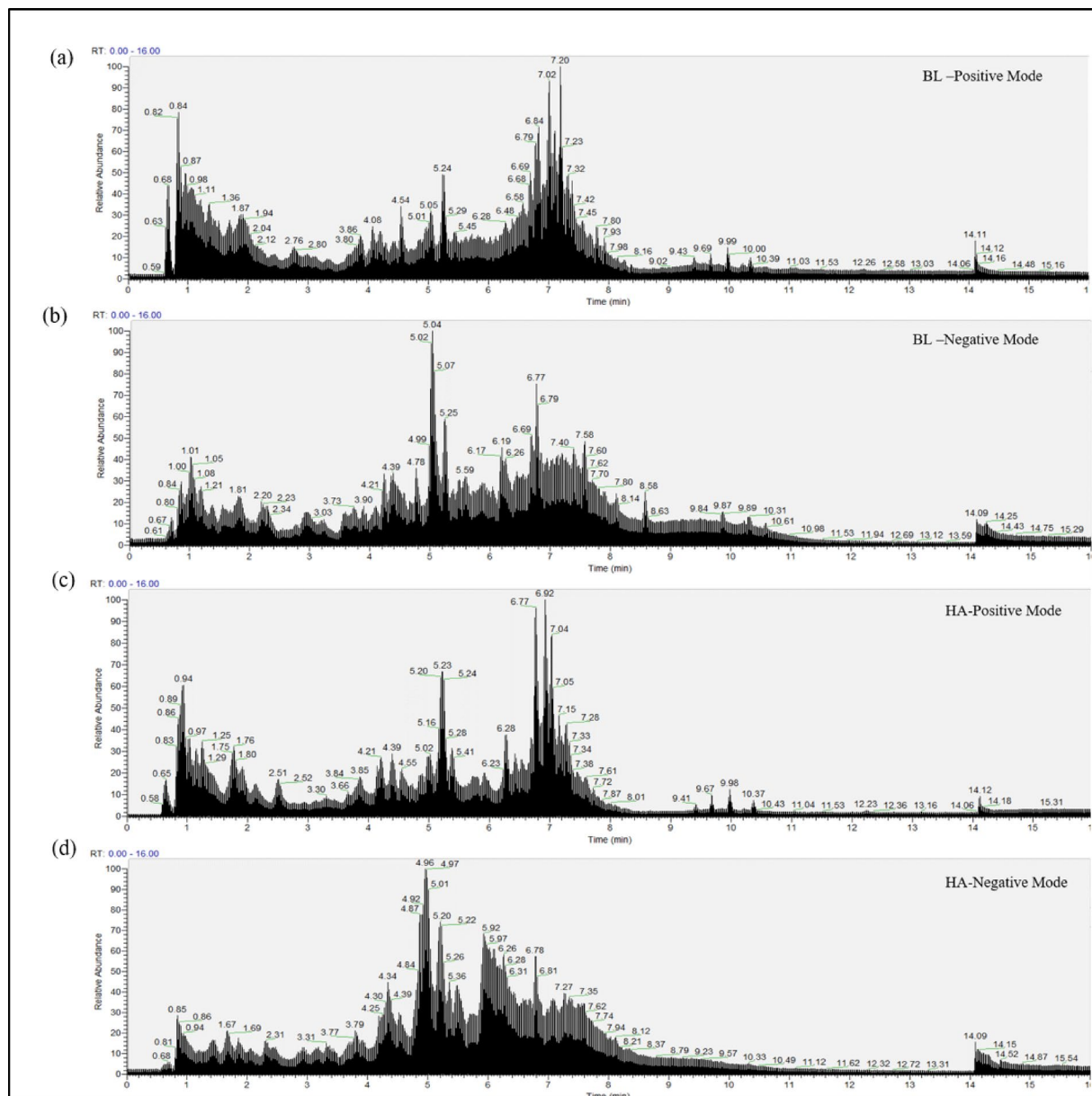


Fig. 1. Representative total ion chromatograms of urine samples separated by LC-MS. (a) Base level, positive mode, (b) base level, negative mode, (c) high-altitude, positive mode, and (d) high-altitude, negative mode.

Selection of differential metabolites in human urine at HA

In the present study, we applied three types of criteria to identify the significantly altered metabolites between groups. First, VIP scores were extracted from the OPLS-DA model and the VIP plot was generated (Fig. 3a, Table S2). Second, for the identification of upregulated and downregulated metabolites, a volcano plot was constructed ($FC > 2$ and < 0.5). According to the volcano plot, there were 20 significantly upregulated metabolites (marked as red dots) and 13 downregulated metabolites (marked as blue dots) (Fig. 3b, Table S4). Third, univariate analysis (t-test) was used to compute the statistical significance as a p-value (Table S3), revealing a total of 33 metabolites highlighted as differentially abundant metabolites. The final results of the selected differentially abundant metabolites are presented in Table 1.

Cluster heat map and correlation analysis of differential metabolites in human urine

To identify a correlation between differential metabolites, because strongly correlated metabolites are closely associated with metabolic networks, participate in the same metabolic pathway, or are directly connected through some biochemical reactions. This analysis extends the utility of metabolite profiles to unravel the global regulatory phenomena underlying phenotypes via systems biology approaches. To elucidate this metabolite correlation, a heatmap (Fig. 4, Table S5) was generated with only differentially abundant metabolites ($n = 33$) on the basis of Pearson correlation (coefficient value, $|r| > 0.8$). A heatmap offers an intuitive depiction of the data,

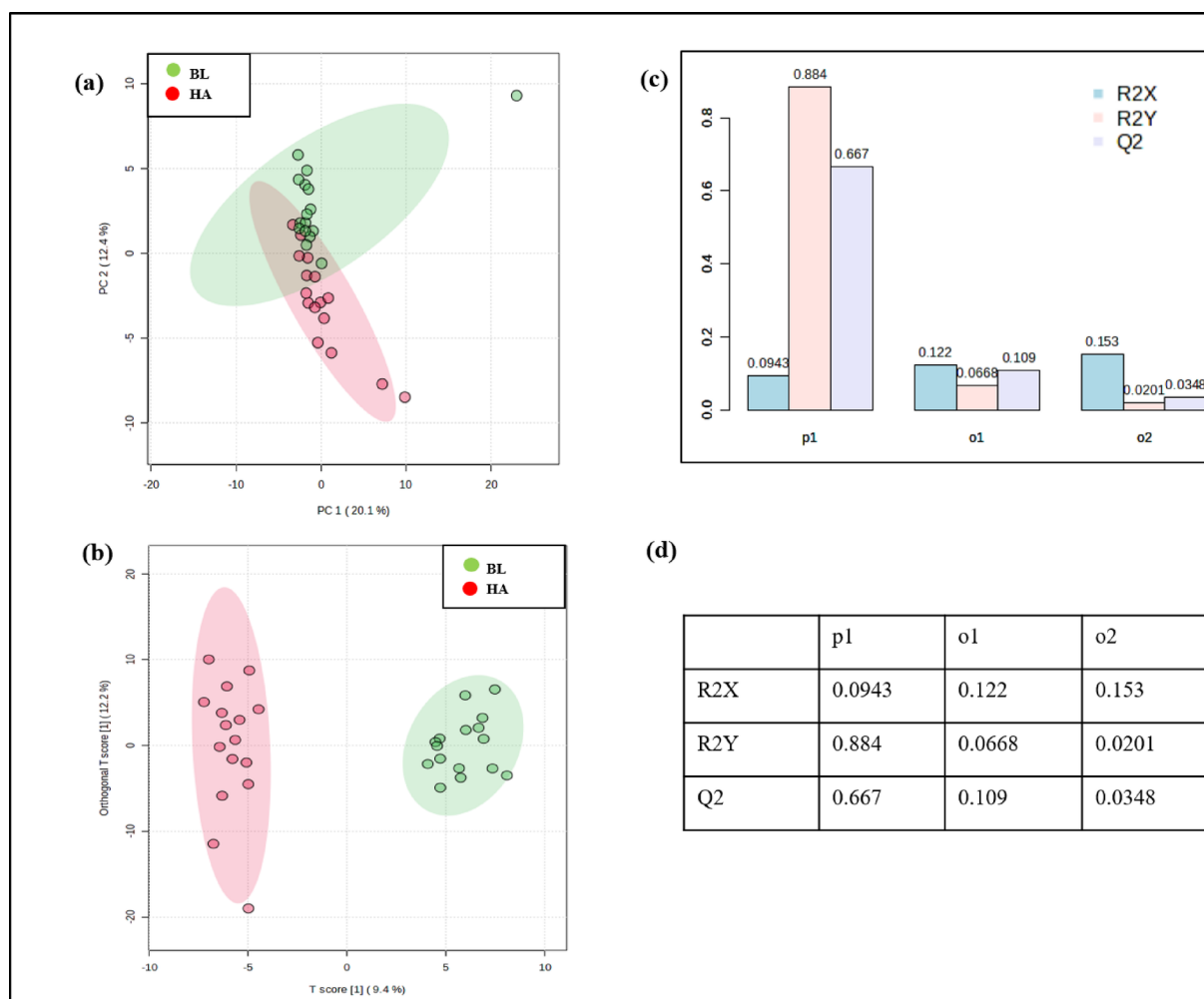


Fig. 2. Metabolomic analysis of HA and BL urine samples was conducted, comprising (a) PCA score plot based on the LC–MS Spectra of urine samples from BL and HA, (b) An OPLS-DA model with logarithmic transformation and Pareto scaling for the metabolomics profiling of urine samples, and (c) OPLS-DA Model validation via a permutation test employing $n = 20$ permutations. (d) Goodness-of-fit parameters generated from the OPLS-DA model, with one predictive (p1) and two orthogonal (o1, and o2) components.

with each colored cell representing the log-normalized concentration of the metabolites within the dataset. The Pearson correlation coefficient (r) served as an index to evaluate the correlation among biological replicates, where r values near 1 signify a robust correlation between the samples. A significance level of $p < 0.05$ was used to determine statistically significant correlations. The results revealed that *N*-Acetyl-S-2-hydroxyethyl-L-cysteine was significantly ($p < 0.0001$) correlated negatively with 4,7-Dihydroxy-2,2-dimethyl-3,4-dihydro-2H-chromen-5-yl hexopyranosiduronic acid ($r = -0.71798$, Dihydrocaffeic acid 3-sulfate ($r = -0.74918$) and 2-Hydroxyacetaminophen sulfate ($r = -0.73505$). The analysis also showed significantly ($p < 0.0001$) positive correlation of 2-Tetrahydrothiopheneacetic acid with Dihomomethionine ($r = 0.85551$), Etilevodopa ($r = 0.81039$) and 4,4'-Thiobis-2-butanone ($r = 0.8155$) (Table 2).

Pathway analysis of differential abundant metabolites at high-altitude

Metabolic pathway analysis was carried out to gain more insight into these significantly modulated metabolites resulting from high-altitude hypoxia utilizing Kyoto Encyclopedia of Genes and Genomes (KEGG) analysis was used to identify metabolic pathways influenced by high-altitude hypoxia. Each affected pathway was screened using the following conditions: pathway impact > 0.05 and $p < 0.05$, which were computed by pathway topology analysis. A total of 29 metabolic pathways were found on the basis of the pathway enrichment results (Table S6). Among them, there were 10 pathways whose impact values were > 0.05 , shown in Fig. 5 and Table 3. Two metabolic pathways namely Pentose & glucuronate interconversions and Vitamin B6 metabolism, were significantly enriched.

Moreover, we conducted a quantitative enrichment analysis utilizing the MetaboAnalyst 6.0 pathway enrichment module and its affiliated Small Molecule Pathway Database (SMPDB) to expand the scope of the metabolomic investigation. In the Fig. 6, Table 4 and table S7 showed two significantly altered pathways i.e.,

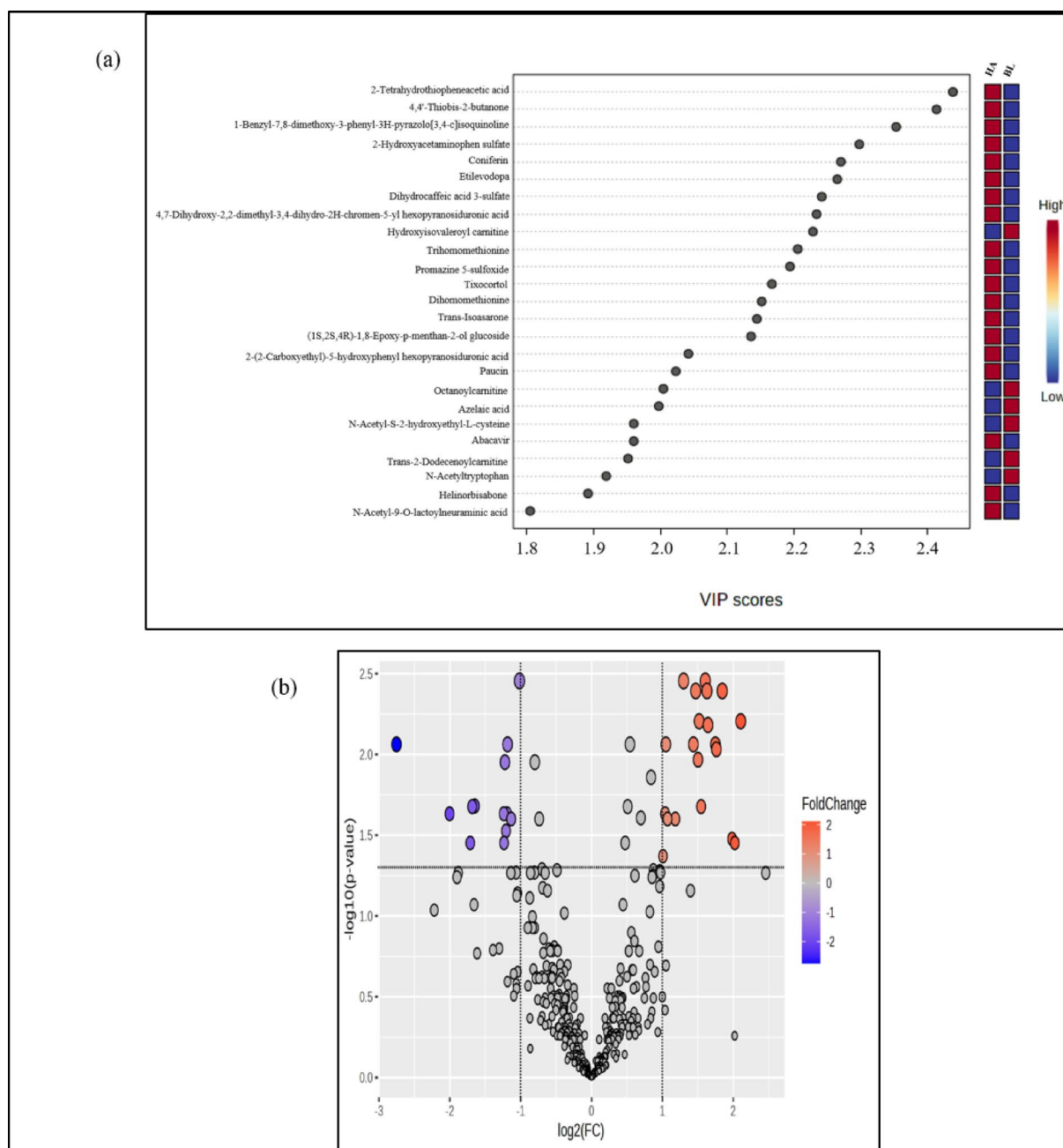


Fig. 3. Differentially abundant metabolite identification and selection. (a) Volcano plot obtained with univariate statistical tests and the magnitude of the change (FC > 2 and < 0.5) in metabolites. Red dots represent the metabolites with p -value < 0.05 and FC > 2. The blue dots represent the metabolites with p -value < 0.05 and FC 0.5. The grey dots represent the metabolites with p -value > 0.05. (b) Top 25 significant features of the metabolite markers based on the VIP projection.

tryptophan metabolism ($p < 0.00437$), catecholamine biosynthesis ($p < 0.0343$), arginine and proline metabolism ($p < 0.0381$) and carnitine synthesis ($p < 0.044$).

Potential biomarker analysis using MetaboAnalyst

To assess the discriminatory ability of the 33 aforementioned differentially expressed metabolites between BL and HA, we used biomarker analysis via the web server MetaboAnalyst 6.0. First, we performed univariate ROC curve analyses for calculation of the Area Under the Curve (AUC), which presented a numerical value description of the relationship between sensitivity and specificity for a given test (Table S8). As presented here, an AUC < 0.5 indicates that the test has no diagnostic value, an AUC of 0.8–0.9 indicates that the test has good accuracy, and an AUC > 0.9 indicates that the diagnostic test has high accuracy. Finally, we obtained five differential metabolites whose AUC values were significantly different between the BL and HA subjects. The

S. No	Metabolites	p Value	FC	VIP
1	Dihydrocaffeic acid 3-sulfate	0.000325	2.067	2.241
2	2-[3,5-dihydroxy-4-(sulfooxy)phenyl]acetic acid	0.001291	2.918	1.386
3	2-Tetrahydrothiopheneacetic acid	5.98E-05	3.589	2.438
4	Promazine 5-sulfoxide	0.000469	2.832	2.194
5	(1S,2S,4R)-1,8-Epoxy-p-menthan-2-ol glucoside	0.000117	4.301	2.135
6	Abacavir	2.69E-05	2.460	1.960
7	Trihomomethionine	0.000332	2.708	2.205
8	Methylxanthine	0.002985	3.950	1.690
9	Abietin	2.21E-05	3.041	2.270
10	p-Coumaric acid sulphate	0.001976	2.269	1.360
11	4,4'-Thiobis-2-butanone	5.80E-05	3.093	2.413
12	2-Hydroxyacetaminophen sulphate	0.000319	3.357	2.297
13	Etilevodopa	6.21E-05	2.770	2.265
14	1-Methyluric acid	0.003521	4.060	1.574
15	Tixocortol	0.000151	3.122	2.167
16	Ecgonine methyl ester	0.004361	2.011	1.801
17	Lycopsamine	0.001622	2.053	1.528
18	4,7-Dihydroxy-2,2-dimethyl-3,4-dihydro-2H-chromen-5-yl hexopyranosiduronic acid	0.0021	2.101	2.234
19	1-Benzyl-7,8-dimethoxy-3-phenyl-3H-pyrazolo[3,4-c]isoquinoline	0.000381	3.390	2.353
20	Dihomomethionine	0.000127	2.863	2.151
21	Dopamine 4-sulfate	1.21E-05	0.494	1.650
22	Azelaic acid	0.002116	0.456	1.997
23	Octanoylcarnitine	0.000275	0.440	2.004
24	Octanoylglucuronide	0.001587	0.437	1.687
25	Desethylchloroquine	0.002584	0.433	1.777
26	2-Hexenoylcarnitine	0.000543	0.429	1.510
27	4-Vinylphenol sulfate	0.003494	0.425	1.663
28	N-Acetyltryptophan	0.00155	0.424	1.919
29	Tetradecanedioic acid	0.00112	0.319	1.673
30	Trans-2-Dodecenoylcarnitine	0.001194	0.311	1.951
31	N-Acetyl-S-2-hydroxyethyl-L-cysteine	0.003307	0.305	1.960
32	N2-Acetylmethionine	0.001668	0.249	1.689
33	Hydroxyisovaleryl carnitine	0.000272	0.148	2.228

Table 1. Differentially abundant metabolites selected between the BL and HA urine samples. FC, fold change; VIP, variable importance in projection.

sensitivity, specificity and area under the curve of the metabolites were as follows: 2-Tetrahydrothiopheneacetic acid (0.9, 0.9, 0.97), 1-Benzyl-7,8-dimethoxy-3-phenyl-3H-pyrazolo[3,4-c]isoquinoline (0.9, 0.9, 0.93), Abietin (0.8, 1, 0.924), 4,4'-Thiobis-2-butanone (0.9, 0.9, 0.922), and Hydroxyisovaleryl carnitine (0.9, 0.9, 0.914) (Fig. 7).

Discussion

Hypoxia experienced at HA exerts a profound and extensive impact on metabolites, eliciting notable alterations in various metabolites and pivotal enzymes. Numerous studies have demonstrated that acute and prolonged exposure to HH results in the physiological responses which include alterations in neurological, cardiac, pulmonary, gastrointestinal, and hematological functions, with adaptations to hypoxia frequently mirrored in the regulatory pathways of associated metabolites^{3,4,22,23}. The current study underscores the comparison of metabolic profiles in urine samples following exposure to physiological, environmental, and psychological stress at BL versus HA. We performed unsupervised, nontargeted LC-MS bases metabolomics to investigate the metabolic alterations, screen differentiated metabolites and metabolic pathways to understand metabolic responses under adaptation/maladaptation to HA stress. First, the PCA score plot illustrated a trend of group clustering allowing visualization of the differentiation of each data point, and representing the metabolic spectrum of every individual between the BL and HA groups (Fig. 2a). Additionally, VIP scores from the OPLS-DA model (Fig. 2b), fold changes from the volcano plot (Fig. 3b), and univariate t-test analysis collectively selected 33 metabolites showing differential expression as shown in Table 1. Subsequent pathway and metabolite enrichment analyses revealed notable alterations in multiple pathways (Figs. 5, 6).

Exposure to HA hypoxia results in many serious neurological concerns, including sleep disturbance, mental and cognitive impairment²⁴. Amino acid metabolism plays significant role in regulating neuronal activity

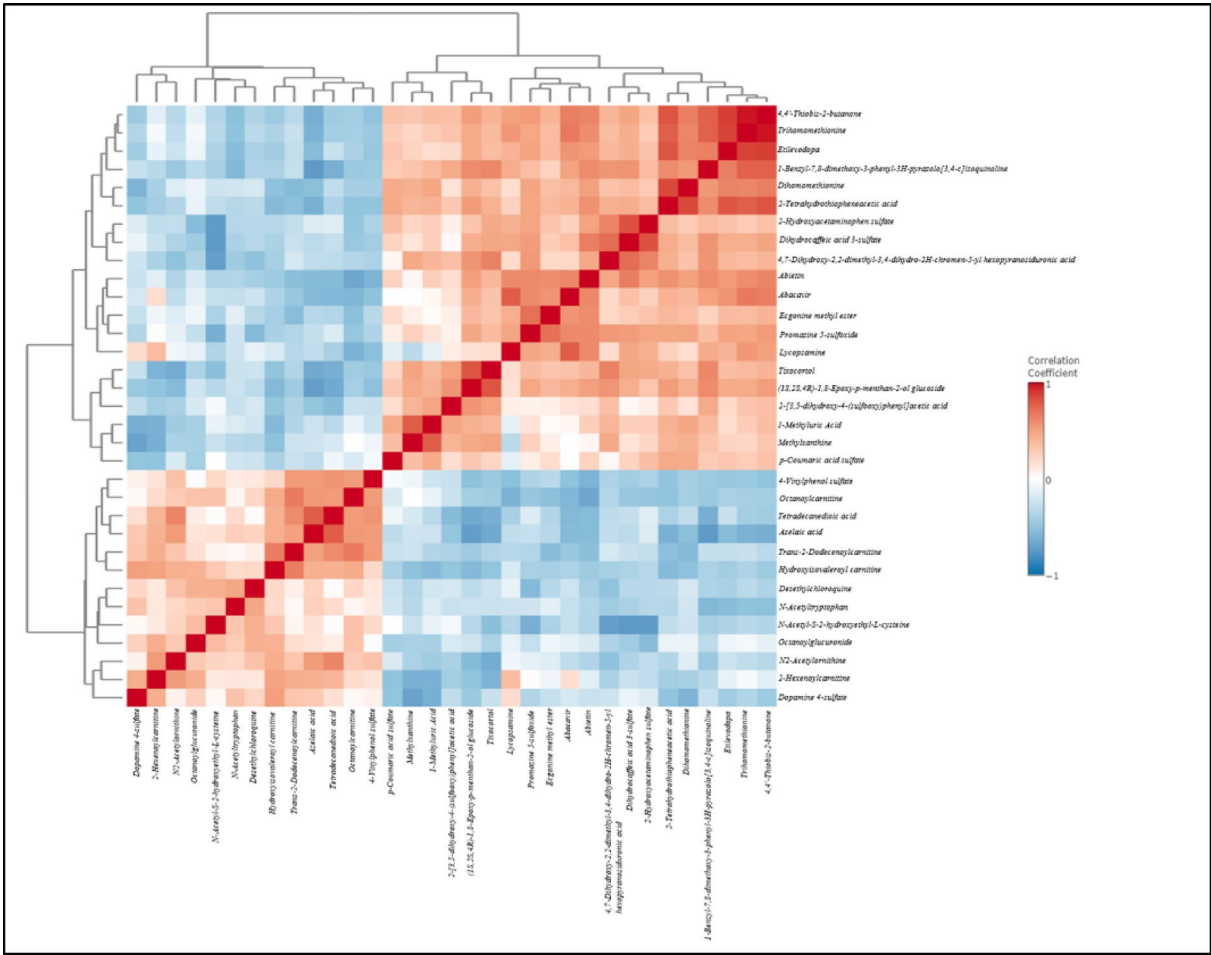


Fig. 4. Heatmap of differential abundant urinary metabolites using pearson (r) correlation. Red boxes represents positive associations and blue boxes represent negative associations between the metabolites.

S. no.	Metabolites		(r)	p value
1	N-Acetyl-S-2 hydroxyethyl-L-cysteine	4,7-Dihydroxy-2,2-dimethyl-3,4-dihydro-2H-chromen-5-yl hexopyranosiduronic acid	−0.717	3.73E−06
		Dihydrocaffeic acid 3-sulfate	−0.749	8.09E−07
		2-Hydroxyacetaminophen sulfate	−0.735	1.66E−06
2	Azelaic acid	(1S,2S,4R)-1,8-Epoxy-p menthan-2-ol glucoside	−0.722	3.03E−06
		1-Benzyl-7,8-dimethoxy-3-phenyl-3H-pyrazolo[3,4-c]isoquinoline	−0.743	1.09E−06
3	(1S,2S,4R)-1,8-Epoxy-p menthan-2-ol glucoside	Tixocortol	0.813	1.53E−08
4	Dihydrocaffeic acid 3-sulfate	2-Hydroxyacetamino	0.826	5.52E−09
5	2 Tetrahydrothiopheneacetic acid	Dihomomethionine	0.855	4.44E−10
		Etilevodopa	0.810	1.90E−08
		4,4'-Thiobis-2-butanone	0.815	1.31E−08
6	Etilevodopa	Trihomomethionine	0.876	5.13E−11
		4,4'-Thiobis-2-butanone	0.885	1.60E−11

Table 2. Pearson correlation matrix between differentially abundant metabolites. r: Correlation coefficient; p value: Statistically significant.

through a variety of mechanisms, ranging from the biosynthesis of neurotransmitters (such as the precursor amino acids phenylalanine, tyrosine and tryptophan) to direct neurotransmission and neuromodulation (such as the excitatory neurotransmitter glutamate and the inhibitory neurotransmitter glycine)^{25,26}. The phenylalanine, tyrosine and tryptophan biosynthesis signalling pathways are related to oxidative stress, the immune response and the regulation of inflammation, and can also be used as energy compensation in extreme environments such as hypoxia⁵. Phenylalanine can be converted into tyrosine, and tyrosine can further produce dopamine,

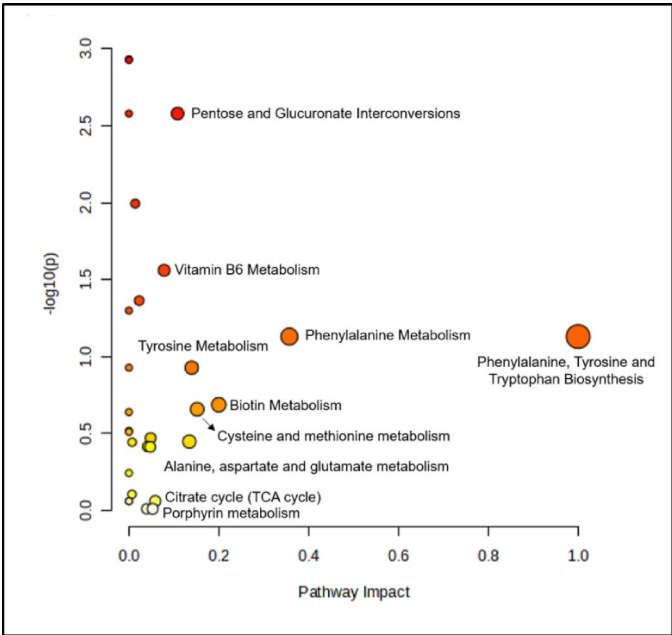


Fig. 5. Bubble plot showing the topology of selected statistically significant metabolites. The horizontal coordinate indicates the pathway impact value, the vertical coordinate indicates the $-\log_{10}(p)$ of the pathway, the bubble area corresponds to the impact of each pathway and the color of the bubble represents significance from red to white, from greatest to least.

S. no.	Pathways	P value	Holm p	FDR	Impact
1	Phenylalanine, tyrosine and tryptophan biosynthesis	0.074	1	0.215	1
2	Phenylalanine metabolism	0.074	1	0.215	0.35
3	Biotin metabolism	0.205	1	0.444	0.2
4	Cysteine and methionine metabolism	0.219	1	0.443	0.15
5	Tyrosine metabolism	0.118	1	0.285	0.13
6	Alanine, aspartate and glutamate metabolism	0.356	1	0.509	0.13
7	Pentose and glucuronate interconversions	0.002	0.07	0.019	0.10
8	Vitamin B6 metabolism	0.027	0.66	0.133	0.07
9	Citrate cycle (TCA cycle)	0.869	1	0.933	0.05
10	Porphyrin metabolism	0.975	1	0.975	0.05

Table 3. Metabolic pathway analysis. Pathway analysis was performed using MetaboAnalyst 6.0. to identify pathways that were significantly altered after HA exposure. Here, p value: The original p value calculated from pathway analysis; Holm p: *p* values adjusted by the Holm–Bonferroni method; FDR, false discovery rate; Impact, represents a combination of the centrality and pathway enrichment result.

norepinephrine and epinephrine. These excitatory neurotransmitters participate in the sleep–wake cycle are important neurotransmitters that cause insomnia and were altered in a recent study²⁷. Several studies have also shown sleep disturbances and periodic breathing (also known as Cheyne–Stokes breathing) in climbers exposed to acute hypoxia at an altitude of 3000 m²⁸. These alterations are increased at very high-altitudes and have been proven via simulated normobaric hypoxia, acute exposure to 4480 m which resulted in a relationship between poor sleep quality and altered mood and cognitive function²⁹. Notably, dysmetabolism of aromatic amino acids leads to changes in the microbial production of phenylalanine and tyrosine derivatives (phenyl carboxylic acid, p-cresol) and tryptophan indole derivatives (indole carboxylic acid, indole) and contributes to pathogenesis in IBS³⁰. These pathways are known for their crucial roles in adaptive and innate immunity³¹ and travelling to HA is associated with increased inflammation³², illness and infection³³ which may be attributed to dysregulation of the immune system.

Biotin serves as a coenzyme for several key enzymes, that play crucial roles in numerous metabolic pathways, including energy metabolism, fatty acid synthesis, and amino acid catabolism. A reduction in biotin levels, as observed in the HA group could affect these metabolic processes, potentially weakening the function of biotin as a coenzyme. Similar results reported in a study in which human metabolites were analysed from plasma samples collected at an altitude of 3650 m⁶. A study provided experimental evidence that exposure to hypobaric hypoxia

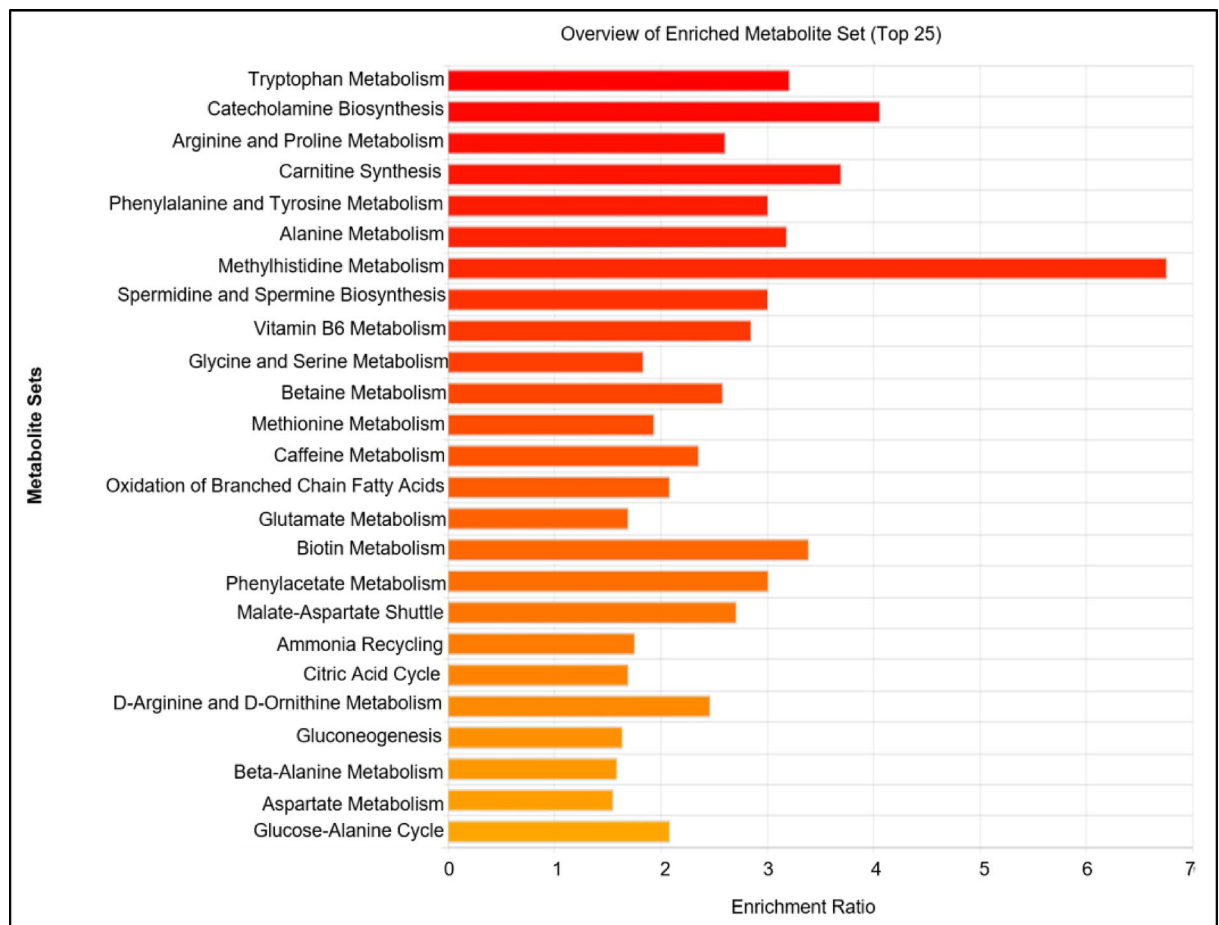


Fig. 6. Quantitative enrichment analysis based on the SMPDB pathway enrichment analysis results for the top 25 metabolic pathways selected via the KEGG database.

S. No	Metabolite set	Total	Hits	Expect	<i>p</i> value	Holm P	FDR
1	Tryptophan metabolism	59	7	2.18	0.004	0.429	0.429
2	Catecholamine biosynthesis	20	3	0.74	0.034	1	1
3	Arginine and proline metabolism	52	5	1.92	0.038	1	1
4	Carnitine synthesis	22	3	0.81	0.044	1	1

Table 4. List of the most significant SMPDB pathways. SMPDB Pathway analysis was performed using MetaboAnalyst 6.0. to identify pathways that were significantly altered after HA exposure. Here, Total: Total number of compounds in the pathways; Hits: Number of compound matched from our data; *p* Value: The original *p* value calculated from pathway analysis; Holm *p*: *p* Values adjusted by the Holm–Bonferroni method; FDR, false discovery rate.

culminates in a marked decrease in the levels of cysteine in both rat brain and human blood samples. This cysteine deficit functionally regulated lowered levels of endogenous H_2S as well as hypobaric hypoxia-induced neuropathological responses in an animal model³⁴. Dysregulated cysteine metabolism is associated with several neurodegenerative disorders. The brain is predominantly vulnerable to high-altitude hypoxia (HAH), and is positively correlated with neurological dysfunction, including cognitive function decline, memory deterioration, paraequilibrium, and somnopathy, which are common symptoms in people who ascend to high-altitude³⁵. A recent case report revealed fronto-temporal neurodegeneration in a 57 year old male who developed symptoms of acute mountain sickness after climbing Mount Everest to 3500 m in Nepal³⁶.

Another important pathway that was altered in our study was the TCA cycle. The TCA cycle is an important source of cellular energy and is involved in numerous cellular metabolic pathways³⁷. Exposure to hypoxia inhibits the TCA cycle pathway and converts the glycolytic pathway into the primary metabolic pathway that generates available energy^{38,39}. Additionally, this cycle has been proven to play a role in erythrocyte metabolism under anoxic conditions⁴⁰. Maimaitiyimin et al. analysed the differences between hypoxia model and normal

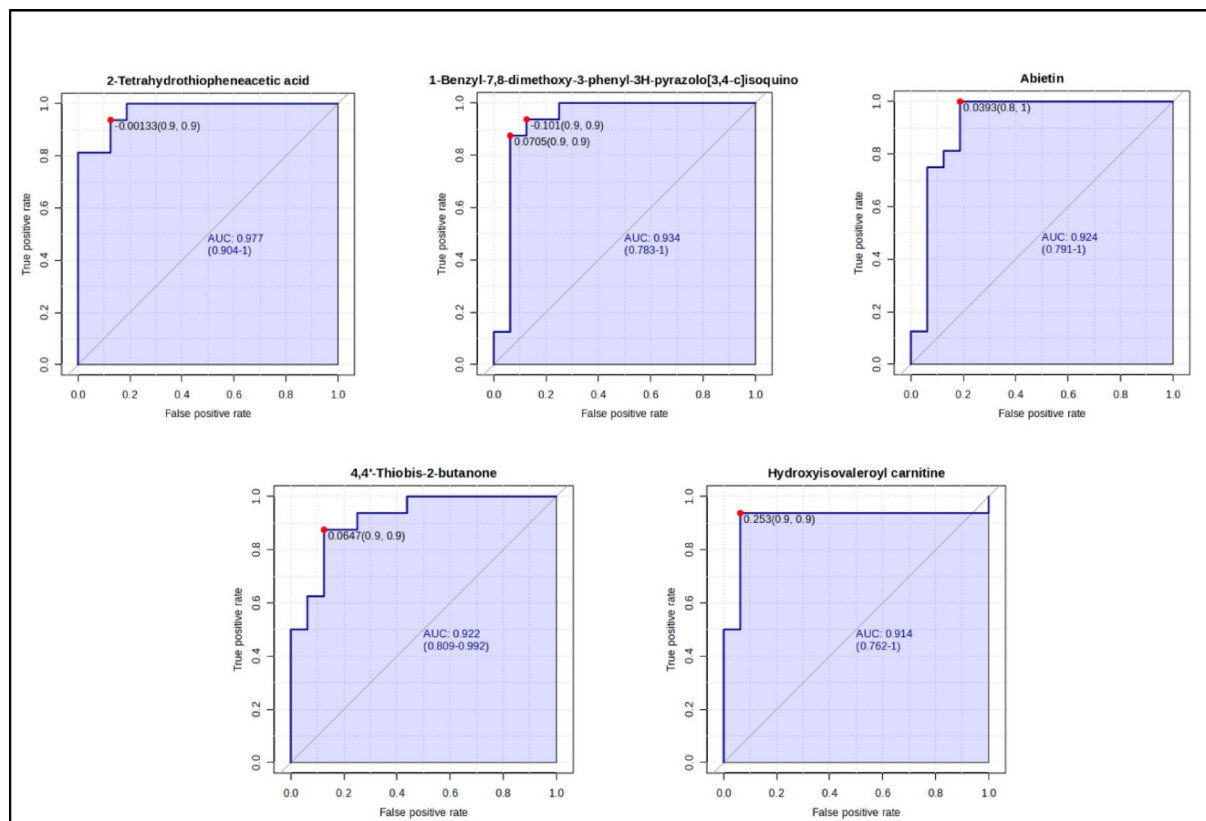


Fig. 7. ROC curve graph. The horizontal coordinates in the graph indicate the positive class rate, i.e. the false positive rate (1-specificity); the vertical coordinates indicate the true class rate, i.e. the true positive rate (sensitivity), and the AUC value, i.e., the area under the curve, the higher the AUC value, i.e., the larger the AUC is, the higher the prediction accuracy. The closer the curve is to the upper left corner (i.e., the smaller X and the larger Y is), the higher the prediction accuracy.

rats and reported that endogenous substances related to energy metabolism were disturbed and that amino acid levels were significantly increased in the hypoxia group⁴¹. Alterations in energy metabolism pathways after HA exposure may contribute to AMS susceptibility at HA⁷. Glutamate, aspartate, L & D alanine, and amino acids are derived from intermediates of the TCA cycle. A previous study identified out alanine, aspartate and glutamate metabolism as potential target pathways for HAPE in patients who developed the disease after travelling from the lowlands to Golmud district (2780–4500 m) in Qinghai, China⁴². Similar observations were made in other studies in which metabolic pathway alterations were observed in microvascular endothelial cells in response to hypoxia⁴³.

Vitamin B6, a component of coenzymes in human body, is involved in various metabolic reactions, especially the metabolism of amino acids such as heme metabolism and tryptophan metabolism^{44,45}. It is a required cofactor for glycogen phosphorylase, which converts stored glycogen into glucose, and is essential for the conversion of various amino acids into oxaloacetate as well as the conversion of α -ketoglutarate, succinyl-CoA, and pyruvate into various amino acids⁴⁶. Vitamin B6 deficiency can lead to increased homocysteine levels, a known risk factor for the development of atherosclerotic cardiovascular disease⁴⁷. In addition to its role in glycogen and amino acid metabolism, two of the major forms of vitamin B6, pyridoxal 5'-phosphate (PLP) and pyridoxal (PL), appear to affect the erythrocyte hemoglobin oxygen binding affinity, with PLP reducing the binding affinity and PL increasing the affinity⁴⁸. These effects, which have been observed only in-vitro and not yet confirmed in vivo, could have effect at high-altitudes, either lowering the ability of hemoglobin to bind sufficient oxygen in the lungs or of increasing the binding affinity to such an extent that the release of the bound oxygen in the peripheral capillary beds is diminished. Pentose and glucuronate interconversion pathway play important roles in many biosynthetic pathways such as gluconeogenesis, transamination, deamination and lipogenesis. This pathway also plays an important role in the removal of bilirubin from the body⁴⁹. Therefore, any error in pentose and glucuronate interconversions will lead to an increase in the level of bilirubin in serum, and the obvious clinical manifestation is that the skin and mucosa are as yellow as orange⁵⁰. There is a hematologic response to decreased oxygen availability at high-altitude, resulting in increased bilirubin production accompanied by delayed bilirubin clearance⁵¹. Excessive bilirubin can enter the brain via the blood–brain barrier to induce neurologic damage⁵².

To determine whether the differentially abundant metabolites that were selected could be used as biomarkers, we performed ROC curve analysis (Fig. 7). According to the ROC, the AUC values of the 5 metabolites in the

two comparisons were relatively high (>0.903). Using metabolomics, we can identify unbiased metabolic profiles of small molecules in urine, which may predict the risk of AMS and HAPE, common HA related illnesses^{7,36,53}. Through the use of multivariate statistics and machine learning algorithms, our study offers novel insights into the domain of high-altitude medicine, shedding light on the associated health issues stemming from exposure to high-altitudes.

Conclusions and future directions

This longitudinal study examined alterations in human urine metabolites after hypobaric hypoxia exposure at HA. Analysis of the urinary metabolomics from the subjects ascending to the high-altitude (4200 m) was compared with their BL urinary metabolomic profiling for the first time. The study revealed significant shifts in metabolism due to high-altitude hypoxic exposure, with numerous metabolites showing differential expression. These differential metabolites hold promise as potential biomarkers for the early detection of high-altitude-induced illnesses. Notably, five potential biomarkers demonstrated significant differences between the BL and HA group, suggesting a lasting effect of high-altitude hypoxia on cellular metabolism. Furthermore, future work should explore the relationship among altitude, urinary metabolites and altitude induces symptoms or diseases with follow-up after travelling or stay at HA with larger cohorts.

Merits and limitations

The strength of current study lies in its longitudinal design, albeit with a restricted number of participants, resulting in limited statistical power. Due to logistical constraints, the small sample size was unavoidable. Follow up studies using a larger sample sizes will be required to validate the biomarker potential. Additionally, the study exclusively involved only male participants. Follow-up analysis was hindered by the unavailability and reluctance of participants to provide urine samples upon returning to the base level (210 m).

Data availability

These data are available at the NIH Common Fund's National Metabolomics Data Repository (NMDR) website, the Metabolomics Workbench (<https://www.metabolomicsworkbench.org>) where it has been assigned Project ID: PR002072. The data can be accessed directly via Project <https://doi.org/10.21228/M8SF9X>.

Received: 8 August 2024; Accepted: 28 April 2025

Published online: 15 May 2025

References

1. Virués-Ortega, J., Buela-Casal, G., Garrido, E. & Alcázar, B. Neuropsychological functioning associated with high-altitude exposure. *Neuropsychol. Rev.* **14**, 197–224 (2004).
2. Davison, G. et al. Metabolomic response to acute hypoxic exercise and recovery in adult males. *Front. Physiol.* **9**, 384408 (2018).
3. Liao, W. T. et al. Metabolite modulation in human plasma in the early phase of acclimatization to hypobaric hypoxia. *Sci. Rep.* **6**(1), 22589 (2016).
4. O'Brien, K. A. et al. Metabolomic and lipidomic plasma profile changes in human participants ascending to Everest Base Camp. *Sci. Rep.* **9**(1), 2297 (2019).
5. Gandhi, S., Chinnadurai, V., Bhadra, K., Gupta, I. & Kanwar, R. S. Urinary metabolic modulation in human participants residing in Siachen: A 1H NMR metabolomics approach. *Sci. Rep.* **12**(1), 9070 (2022).
6. Zhu, G. et al. Metabolomic analysis of plasma from patients with acute mountain sickness using chromatography–mass spectrometry. *Medicine* **94**(45), e1988 (2015).
7. Sibomana, I. et al. Urinary metabolites as predictors of acute mountain sickness severity. *Front. Physiol.* **12**, 709804 (2021).
8. Lindon, J. C., Nicholson, J. K., Holmes, E. & Everett, J. R. Metabonomics: metabolic processes studied by NMR spectroscopy of biofluids. *Conc. Magn. Reson.: Educ. J.* **12**(5), 289–320 (2000).
9. Serkova, N. J. & Niemann, C. U. Pattern recognition and biomarker validation using quantitative 1H-NMR-based metabolomics. *Expert Rev. Mol. Diagn.* **6**(5), 717–731 (2006).
10. Bhushan, B. et al. Urine metabolite profiling of Indian Antarctic Expedition members: NMR spectroscopy-based metabolomic investigation. *Heliyon* **7**(5), e07114 (2021).
11. Bouatra, S. et al. The human urine metabolome. *PLoS ONE* **8**(9), e73076 (2013).
12. Emwas, A. H. et al. Recommendations and standardization of biomarker quantification using NMR-based metabolomics with particular focus on urinary analysis. *J. Proteome Res.* **15**(2), 360–373 (2016).
13. Miller, I. J. et al. Real-time health monitoring through urine metabolomics. *NPJ Digit. Med.* **2**(1), 109 (2019).
14. Elliott, P. et al. Urinary metabolic signatures of human adiposity. *Sci. Transl. Med.* **7**(285), 285ra62 (2015).
15. Van Duynhoven, J. P. & Jacobs, D. M. Assessment of dietary exposure and effect in humans: the role of NMR. *Prog. Nucl. Magn. Reson. Spectrosc.* **96**, 58–72 (2016).
16. Liu, X. & Locasale, J. W. Metabolomics: A primer. *Trends Biochem. Sci.* **42**(4), 274–284 (2017).
17. Sajid, M. I. et al. Untargeted metabolomics analysis on kidney tissues from mice reveals potential hypoxia biomarkers. *Sci. Rep.* **13**(1), 17516 (2023).
18. Patterson, A. D., Gonzalez, F. J. & Idle, J. R. Xenobiotic metabolism: A view through the metabolometer. *Chem. Res. Toxicol.* **23**(5), 851–860 (2010).
19. Bajad, S. & Shulaev, V. Highly-parallel metabolomics approaches using LC-MS2 for pharmaceutical and environmental analysis. *Trends Anal. Chem.* **26**(6), 625–636 (2007).
20. Wishart, D. S. et al. HMDB 5.0: The human metabolome database for 2022. *Nucleic Acids Res.* **50**(D1), 622–631 (2022).
21. Ewald, J. D. et al. Web-based multi-omics integration using the Analyst software suite. *Nat. Protoc.* **19**, 1467 (2024).
22. Serkova, N. J., Reisdorff, N. A. & Tissot van Patot, M. C. Metabolic markers of hypoxia: Systems biology application in biomedicine. *Toxicol. Mech. Methods* **18**(1), 81–95 (2008).
23. Zhu, G. et al. Metabolomic analysis of plasma from patients with acute mountain sickness using chromatography–mass spectrometry. *Medicine* **94**(45), 1988 (2015).
24. Bartscher, J., Mallet, R. T., Bartscher, M. & Millet, G. P. Hypoxia and brain aging: Neurodegeneration or neuroprotection? *Ageing Res. Rev.* **68**, 101343 (2021).

25. Vallianatou, T., Bèchet, N. B., Correia, M. S. P., Lundgaard, I. & Globisch, D. Regional Brain analysis of modified amino acids and dipeptides during the sleep/wake cycle. *Metabolites* **12**, 21 (2021).
26. Dalangin, R., Kim, A. & Campbell, R. E. The role of amino acids in neurotransmission and fluorescent tools for their detection. *Int. J. Mol. Sci.* **21**(17), 6197 (2020).
27. Wen, Q. et al. Urine metabolomics analysis of sleep quality in deep-underground miners: A pilot study. *Public Health Front.* **10**, 969113 (2022).
28. Waggner, T. B., Brusil, P. J., Kronauer, R. E., Gabel, R. A. & Inbar, G. F. Strength and cycle time of high-altitude ventilatory patterns in unacclimatized humans. *J. Appl. Physiol.* **56**(3), 576–581 (1984).
29. de Aquino Lemos, V. et al. High altitude exposure impairs sleep patterns, mood, and cognitive functions. *Psychophysiology* **49**(9), 1298–1306 (2012).
30. Sitkin, S. I., Tkachenko, E. I. & Vakhitov, T. Y. Metabolic dysbiosis of the gut microbiota and its biomarkers. *Clin. Exp. Gastroenterol.* **12**(12), 6–29 (2016).
31. Chen, Q. et al. Integrative analysis of metabolomics and proteomics reveals amino acid metabolism disorder in sepsis. *J. Transl. Med.* **20**(1), 123 (2022).
32. Pham, K., Parikh, K. & Heinrich, E. C. Hypoxia and inflammation: insights from high-altitude physiology. *Front. Physiol.* **12**, 676782 (2021).
33. Khanna, K., Mishra, K. P., Ganju, L., Kumar, B. & Singh, S. B. High-altitude-induced alterations in gut-immune axis: A review. *Int. Rev. Immunol.* **37**(2), 119–126 (2018).
34. Mishra, S. et al. Cysteine becomes conditionally essential during hypobaric hypoxia and regulates adaptive neuro-physiological responses through CBS/H2S pathway. *Biochim. Biophys. Acta Mol. Basis Dis.* **1866**(7), 165769 (2020).
35. Golpich, M. et al. Mitochondrial dysfunction and biogenesis in neurodegenerative diseases: Pathogenesis and treatment. *CNS Neurosci. Ther.* **23**(1), 5–22 (2017).
36. Tunalı, C. H., Ünal, S. & Kamlı, S. A frontotemporal dementia-like case after high-altitude climbing. *Egypt. J. Neurol. Psych.* **59**(1), 10 (2023).
37. Ahn, C. S. & Metallo, C. M. Mitochondria as biosynthetic factories for cancer proliferation. *Cancer Metab.* **3**, 1–10 (2015).
38. Kang, W., Suzuki, M., Saito, T. & Miyado, K. Emerging role of TCA cycle-related enzymes in human diseases. *Int. J. Mol. Sci.* **22**(23), 13057 (2021).
39. Fuller, G. G. & Kim, J. K. Compartmentalization and metabolic regulation of glycolysis. *J. Cell Sci.* **134**(20), jcs258469 (2021).
40. Gao, Y. et al. Transcriptomics and metabolomics study in mouse kidney of the molecular mechanism underlying energy metabolism response to hypoxic stress in highland areas. *Exp. Ther. Med.* **26**(5), 1–17 (2023).
41. Nemkov, T. et al. Metabolism of citrate and other carboxylic acids in erythrocytes as a function of oxygen saturation and refrigerated storage. *Front. Med.* **4**, 175 (2017).
42. Guo, L. et al. Three plasma metabolite signatures for diagnosing high altitude pulmonary edema. *Sci. Rep.* **5**(1), 15126 (2015).
43. Cohen, E. B., Geck, R. C. & Toker, A. Metabolic pathway alterations in microvascular endothelial cells in response to hypoxia. *PLoS ONE* **15**(7), e0232072 (2020).
44. Mitchell, D., Wagner, C., Stone, W. J., Wilkinson, G. R. & Schenker, S. Abnormal regulation of plasma pyridoxal 5'-phosphate in patients with liver disease. *Gastroenterology* **71**(6), 1043–1049 (1976).
45. Bitetto, D. et al. Complementary role of vitamin D deficiency and the interleukin-28B rs12979860 C/T polymorphism in predicting antiviral response in chronic hepatitis C. *Hepatology* **53**(4), 1118–1126 (2011).
46. Parra, M., Stahl, S. & Hellmann, H. Vitamin B6 and its role in cell metabolism and physiology. *Cells* **7**(7), 84 (2018).
47. Brown, M. J., Ameer, M. A. & Beier, K. *Vitamin B6 Deficiency* (Starpearls Publishing, 2017).
48. Reynolds, R. D., Marriott, B. M. & Carlson, S. J. *Effects of cold and altitude on vitamin and mineral requirements* 189–202 (National Academies Press (US), 1996).
49. Fang, H. et al. Insight into the metabolic mechanism of scoparone on biomarkers for inhibiting Yanghuang syndrome. *Sci. Rep.* **6**(1), 37519 (2016).
50. He, Y. et al. Metabolomics analysis coupled with UPLC/MS on therapeutic effect of jigucao capsule against dampness-heat jaundice syndrome. *Front. Pharmacol.* **13**, 822193 (2022).
51. Memon, N., Weinberger, B. I., Hegyi, T. & Aleksunes, L. M. Inherited disorders of bilirubin clearance. *Pediatr. Res.* **79**(3), 378–386 (2016).
52. Pranty, A. I., Shumka, S. & Adjaye, J. Bilirubin-induced neurological damage: current and emerging iPSC-derived brain organoid models. *Cells* **11**(17), 2647 (2022).
53. Luo, Y., Zhu, J. & Gao, Y. Metabolomic analysis of the plasma of patients with high-altitude pulmonary edema (HAPE) using 1H NMR. *Mol. Biosyst.* **8**(6), 1783–1788 (2012).

Acknowledgements

We are thankful to the Directors, Defence Institute of Physiology and Allied Sciences (DIPAS) for their guidance and financial support the study. The authors are also thankful to Ms. Harshita Gupta, Technician 'B' Department of Disruptive and Deterrence Technologies. We also thank DIPAS-DRDO for their constant technical and logistic support during the course of this study. Additionally, Valerian Info Pvt. Ltd is greatly acknowledged for data assembly and analysis. All the subjects are accredited for participating in the study. MK is supported by a fellowship from UGC-CSIR, Ministry of Human Resources, Government of India, Delhi, India. DS is supported by a fellowship from DIPAS-DRDO, Ministry of Defence, Government of India, Delhi, India.

Author contributions

RCM and LG designed the project, study protocol and supervised all collection during the project. MPKR obtained the Human Ethical Clearance and provided logistic support at high-altitude. MRE collected the sample at base level and high-altitude. MK, AK, DS and CR carried out the data collection, literature survey and data interpretation. RCM and MK performed the data analysis, interpretation, discussion and wrote the manuscript. RCM and RV reviewed and approved the final manuscript.

Funding

This work is supported by the Defence Institute of Physiology and Allied Sciences, Defence Research and Development Organization, Delhi-110054, India.

Declarations

Competing interests

The authors declare no competing interests.

Additional information

Supplementary Information The online version contains supplementary material available at <https://doi.org/10.1038/s41598-025-00312-y>.

Correspondence and requests for materials should be addressed to R.C.M.

Reprints and permissions information is available at www.nature.com/reprints.

Publisher's note Springer Nature remains neutral with regard to jurisdictional claims in published maps and institutional affiliations.

Open Access This article is licensed under a Creative Commons Attribution-NonCommercial-NoDerivatives 4.0 International License, which permits any non-commercial use, sharing, distribution and reproduction in any medium or format, as long as you give appropriate credit to the original author(s) and the source, provide a link to the Creative Commons licence, and indicate if you modified the licensed material. You do not have permission under this licence to share adapted material derived from this article or parts of it. The images or other third party material in this article are included in the article's Creative Commons licence, unless indicated otherwise in a credit line to the material. If material is not included in the article's Creative Commons licence and your intended use is not permitted by statutory regulation or exceeds the permitted use, you will need to obtain permission directly from the copyright holder. To view a copy of this licence, visit <http://creativecommons.org/licenses/by-nc-nd/4.0/>.

© The Author(s) 2025